Research Article

Rapid Communications in Mass Spectrometry

Received: 17 January 2013 Revised: 31 January 2013 Accepted: 1 February 2013 Published online in Wiley Online Library

Rapid Commun. Mass Spectrom. **2013**, 27, 993–1004
(wileyonlinelibrary.com) DOI: 10.1002/rcm.6539

Monitoring phosphodiesterase-4 inhibitors using liquid chromatography/(tandem) mass spectrometry in sports drug testing

Mario Thevis[1,2]*, Oliver Krug[1,2] and Wilhelm Schänzer[1]

[1]Institute of Biochemistry - Center for Preventive Doping Research, German Sport University Cologne, Am Sportpark Müngersdorf 6, 50933 Cologne, Germany
[2]European Monitoring Center for Emerging Doping Agents, Cologne/Bonn, Germany

RATIONALE: The recent discovery of resveratrol's capability to inhibit cAMP-specific phosphodiesterases (PDEs) and, as a consequence, to enhance particularly the activity of Sirt1 in animal models has reinforced the interest of preventive doping research organizations, especially in PDE4 inhibitors. Among these, the archetypical PDE4-inhibitor rolipram significantly increased the number of mitochondria in laboratory rodents, which further demonstrated a performance increase in a treadmill-test (time-to-exhaustion) of approximately 40%. Besides rolipram, a variety of new PDE4-inhibiting substances including cilomilast, roflumilast, and numerous additional new drug entities were described, with roflumilast being the first-in-class having received clinical approval for the treatment of chronic obstructive pulmonary disease (COPD). Due to the availability of these substances, and the fact that a misuse of such compounds in sport cannot be excluded, it deems relevant to probe for the prevalence of these compounds in sports drug testing programs.
METHODS: Known urinary phase-I metabolites of rolipram, roflumilast, and cilomilast were generated by *in vitro* incubations employing human liver microsomal preparations. The metabolites obtained were studied by liquid chromatography with high-resolution/high-accuracy tandem mass spectrometry (LC/MS/MS) and the reference product ion mass spectra of established and most relevant metabolites were utilized to provide the information necessary for comprehensive doping controls. The analytical procedure was based on conventional routine doping control assays employing enzymatic hydrolysis followed by liquid–liquid extraction and subsequent LC/MS/MS measurement.
RESULTS: Structures of diagnostic product ions and dissociation pathways of target analytes were elucidated, providing the information required for implementation into an existing test method for routine sports drug testing. The established method allowed for detection limits for the intact drugs of 1–5 ng/mL, and further assay characteristics (intraday precision 1.5–13.7%, interday precision 7.3–18.6%, recovery 20–100%, ion suppression/enhancement, and specificity) were determined. In addition, proof-of-concept analyses concerning roflumilast were conducted with a urine sample obtained from a COPD patient under roflumilast treatment. Copyright © 2013 John Wiley & Sons, Ltd.

The search for resveratrol's route of action concerning its ability to mimic calorie restriction has led to numerous controversies and debates, resulting in comprehensive research programs, particularly targeting mammalian sirtuins.[1] Very recently, the inhibiting effect of resveratrol on phosphodiesterase 4 (PDE4) (Fig. 1 (**1**)), which interferes with the conversion of 3′-5′-cyclic adenosine monophosphate (cAMP) into AMP, was discovered and has since been considered the missing piece of the puzzle allowing explanation of the beneficial effects of resveratrol (e.g. extended life span and improved fat utilization) in animal test models.[2,3] Comprehensive and detailed follow-up studies concerning the cascade of consequences associated with PDE4 inhibition, particularly in muscle cells, corroborated the postulated mechanisms that eventually result in increased mitochondrial biogenesis and function associated with improved fat utilization and, last but not least, enhanced exercise performance. Employing synthetic PDE4-specific substances such as rolipram (Fig. 1 (**2**)), an archetypical PDE4 inhibitor, comparable effects were observed, transferring approved drugs and drug candidates of this category inevitably into the focus of sports drug testing and preventive doping research organizations. Besides rolipram, a considerable number of at least 50 candidates has been introduced as potential therapeutic agents;[4] however, to date only one (roflumilast, Fig. 1 (**3**)) has received clinical approval for the treatment of chronic obstructive pulmonary disease (COPD),[5,6] the field of particular relevance for PDE4 inhibition.[7–9] Further, cilomilast (Fig. 1 (**4**)) has advanced to phase-III clinical trials[10] and various alternative structures in pre-clinical or early clinical development have recently been summarized in a comprehensive review.[4]

In the present study, the mass spectrometric characterization of the PDE4 inhibitors rolipram, roflumilast, cilomilast, and corresponding phase-I and phase-II metabolic products by means of high-resolution/high-accuracy mass spectrometry (MS) has been reported. In order to efficiently screen for

* *Correspondence to:* M. Thevis, Institute of Biochemistry - Center for Preventive Doping Research, German Sport University Cologne, Am Sportpark Müngersdorf 6, 50933 Cologne, Germany.
E-mail: m.thevis@biochem.dshs-koeln.de

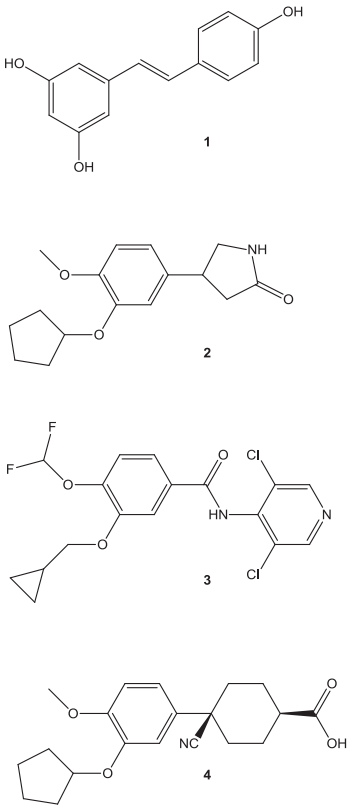

Figure 1. Chemical structures of (1) resveratrol ($C_{14}H_{12}O_3$, mol wt = 228), (2) rolipram ($C_{16}H_{21}NO_3$, mol wt = 275), (3) roflumilast ($C_{17}H_{14}Cl_2F_2N_2O_3$, mol wt = 402), and (4) cilomilast ($C_{20}H_{25}NO_4$, mol wt = 343).

compounds potentially relevant for sports drug testing, preventive and proactive measures are required that necessitate detailed knowledge concerning the analytes' physicochemical properties and, among these, especially ionization and dissociation behavior under different analytical conditions. The pharmacokinetic profiles, metabolism and disposition of rolipram (**2**), roflumilast (**3**), and cilomilast (**4**) in humans have been described previously,[6,10–14] but only little has been published on mass spectral data concerning the active drugs and respective metabolic products,[15] particularly those extracted from urine. Established metabolites were prepared by *in vitro* incubations employing human liver microsomal preparations, and their dissociation pattern was elucidated under electrospray ionization (ESI) and collision-induced dissociation (CID) conditions. Subsequently, existing routine doping control assays were validated to allow for the inclusion of the characterized analytes, and proof-of-concept data were obtained for roflumilast by the analysis of a urine sample collected from a patient undergoing COPD treatment.

EXPERIMENTAL

Chemicals and reagents

Reference material of rolipram, deuteroxide and methanol-D_1 was obtained from Sigma (Schnelldorf, Germany), roflumilast was from Takeda GmbH (Konstanz, Germany), and cilomilast from Selleckchem (Munich, Germany). Human liver microsomal and S9 enzymes were purchased from BD Gentest (Woburn, MA, USA), nicotinamide adenine dinucleotide phosphate (NADPH) and *ß*-glucuronidase (*E. coli*) from Roche Diagnostics (Mannheim, Germany). Deionized water was used for all aqueous buffers and all organic solvents (Merck, Darmstadt, Germany) were of analytical grade.

Electrospray ionization (tandem) mass spectrometry and liquid chromatography-ESI-MS/MS

High-resolution/high-accuracy ESI-MS/MS was conducted using an AB Sciex TripleTOF 5600 instrument (Darmstadt, Germany) equipped with a DuoSpray ion source operated at 25 °C and 5000 V. The mass spectrometer was calibrated using the manufacturer's protocol allowing for mass accuracies < 6 ppm for the period of analysis. A minimum of 30 spectra were averaged to calculate the accurate masses of target ions. The declustering potential was set to 100 V and collision offset voltages were optimized to retain approximately 10−20% of relative abundance of the precursor ion. Nitrogen was used as the collision and the curtain gas supplied by a nitrogen generator (CMC Instruments, Eschborn, Germany). Working solutions of the analytes were introduced via a syringe pump at a flow rate of 10 µL/min.

Analyses requiring MS^3 experiments were conducted on an AB Sciex 5500 QTrap mass spectrometer employing a Turbo V ion source at 25 °C and 5000 V, and the working solutions were infused by means of a syringe pump at 10 µL/min. Collision and excitation energies were adjusted to provide comprehensive information on product ions as well as maintaining approximately 10% (relative abundance) of the respective precursor ion. Collision gas was nitrogen provided by the same CMC N_2-generator mentioned above.

Liquid chromatography with tandem mass spectrometry (LC/MS/MS) was carried out using both above-mentioned MS systems interfaced to an Agilent (Waldbronn, Germany) 1260 LC apparatus equipped with a Macherey-Nagel (Düren, Germany) Pyramid column (50 × 2 mm, particle size 3 µm) using 5 mM ammonium acetate containing 0.1% acetic acid and acetonitrile as solvents A and B, respectively. A flow rate of 250 µL/min was used and gradient elution employed starting at 90% A, decreasing to 0% A within 8 min, maintaining 0% A for another 3 min before returning to starting conditions. The effluent was directed to the Turbo V ion source, which was operated at 500 °C with a capillary voltage of 5500 V. The TripleTOF was run in high-sensitivity mode at a resolution of approximately 23 000 (full width at half maximum (FWHM)) and the 5500 QTrap in either enhanced product ion, MS^3, or multiple reaction monitoring (MRM) mode. In all cases, Q1 was set to unit resolution for precursor ion selection, and for doping control screening purposes (i.e. MRM mode), the collision energies were optimized for each desired ion transition. Selected precursor–product ion pairs with favorable signal-to-noise ratios suitable for routine urine analyses are denoted in Table 1 by bold typeface.

In vitro metabolism studies

In accordance with methods reported earlier,[16,17] *in vitro* metabolic reactions of PDE4 inhibitors were conducted with human liver S9 and microsomal fractions (2 mg/mL final protein concentration) and 100 µM analyte concentration in

Table 1. Elemental compositions of protonated molecules $[M+H]^+$ of rolipram, roflumilast, cilomilast, and corresponding metabolites, with resulting diagnostic product ions, using high-resolution/high-accuracy MS/MS experiments. Product ions potentially useful for routine doping control analyses are denoted in **bold** typeface

Compound	Metabolic reaction	$[M+H]^+$ (*m/z*)	Elemental composition (experimental)	Error (ppm)	CE (eV)	Product ion (*m/z*)	Relative abundance (%)	Elemental composition (experimental)	Error (ppm)	Cleaved species
Rolipram		276.1594	$C_{16}H_{22}O_3N$	1.7	25	208.0971	41	$C_{11}H_{14}O_3N$	1.6	C_5H_8
						191.0704	65	$C_{11}H_{11}O_3$	0.6	C_5H_8, NH_3
						163.0756	40	$C_{10}H_{11}O_2$	1.2	C_5H_8, NH_3, CO
						131.0491	100	C_9H_7O	0.0	C_5H_8, NH_3, CO, CH_3OH
						103.0541	63	C_8H_7	−0.7	C_5H_8, NH_3, CO (2*x*), CH_3OH
M1	Dealkylation (decyclopentylation)	208.0966	$C_{11}H_{14}O_3N$	−0.8	20	**191.0700**	23	$C_{11}H_{11}O_3$	−1.5	NH_3
						163.0754	27	$C_{10}H_{11}O_2$	0.2	NH_3, CO
						131.0491	100	C_9H_7O	0.0	NH_3, CO, CH_3OH
						103.0542	99	C_8H_7	−0.1	NH_3, CO (2*x*), CH_3OH
M2	Dealkylation (demethylation)	262.1431	$C_{15}H_{20}O_3N$	−2.7	25	**194.0812**	74	$C_{10}H_{12}O_3N$	0.0	C_5H_8
						177.0542	73	$C_{10}H_9O_3$	−2.4	C_5H_8, NH_3
						149.0593	65	$C_9H_9O_2$	−3.1	C_5H_8, NH_3, CO
						131.0489	100	C_9H_7O	−2.0	C_5H_8, NH_3, CO, H_2O
						103.0537	58	C_8H_7	−5.5	C_5H_8, NH_3, CO (2*x*), H_2O
M3/M4	Hydroxylation (cyclopentyl residue)	292.1543	$C_{16}H_{22}O_4N$	−0.1	15	274.1441	9	$C_{16}H_{20}O_3N$	1.1	H_2O
						257.1175	11	$C_{16}H_{17}O_3$	1.1	H_2O, NH_3
						208.0968	100	$C_{11}H_{14}O_3N$	0.1	C_5H_8O
						191.0702	65	$C_{11}H_{11}O_3$	−0.6	C_5H_8O, NH_3
						163.0750	32	$C_{10}H_{11}O_2$	−2.4	C_5H_8O, NH_3, CO
						131.0490	49	C_9H_7O	−0.8	C_5H_8O, NH_3, CO, CH_3OH
						103.0539	27	C_8H_7	−3.2	C_5H_8O, NH_3, CO (2*x*), CH_3OH
M5/M6	Hydroxylation (pyrrolidinone residue)	292.1547	$C_{16}H_{22}O_4N$	1.2	15	207.0652	41	$C_{11}H_{11}O_4$	0.1	C_5H_8, NH_3
						189.0547	71	$C_{11}H_9O_3$	0.5	C_5H_8, NH_3, H_2O
						179.0704	55	$C_{10}H_{11}O_3$	0.4	C_5H_8, NH_3, CO
						163.0751	15	$C_{10}H_{11}O_2$	−1.6	C_5H_8, NH_3, CO_2
						161.0597	66	$C_{10}H_9O_2$	0.2	C_5H_8, NH_3, CO, H_2O
						131.0489	68	C_9H_7O	−2.0	C_5H_8, NH_3, CO_2, CH_3OH
						103.0541	100	C_8H_7	−0.9	C_5H_8, NH_3, CO_2, CH_3OH,CO
Roflumilast		403.0435	$C_{17}H_{15}O_3N_2F_2Cl_2$	3.1	20	367.0656	3	$C_{17}H_{14}O_3N_2F_2Cl$	0.1	HCl
						241.0672	79	$C_{12}H_{11}O_3F_2$	0.2	$C_5H_4N_2Cl_2$
						187.0202	100	$C_8H_5O_3F_2$	0.2	$C_5H_4N_2Cl_2$, C_4H_6
						167.0143	6	$C_8H_4O_3F$	1.7	$C_5H_4N_2Cl_2$, C_4H_6, HF

(*Continues*)

Table 1. (Continued)

Compound	Metabolic reaction	$[M+H]^+$ (*m/z*)	Elemental composition (experimental)	Error (ppm)	CE (eV)	Product ion (*m/z*)	Relative abundance (%)	Elemental composition (experimental)	Error (ppm)	Cleaved species
						163.9664	17	$C_5H_4ONCl_2$	−0.4	$C_{12}H_{11}O_2NF_2$
Roflumilast H/D exchange		405.0532	$C_{17}H_{13}D_2O_3N_2F_2Cl_2$	−3.9	20	368.0709	3	$C_{17}H_{13}DO_3N_2F_2Cl$	1.6	DCl
						241.0678	76	$C_{12}H_{11}O_3F_2$	0.0	$C_5H_2D_2N_2Cl_2$
						187.0202	100	$C_8H_5O_3F_2$	0.0	$C_5H_2D_2N_2Cl_2$, C_4H_6
						167.0138	6	$C_8H_4O_3F$	0.5	$C_5H_2D_2N_2Cl_2$, C_4H_6, HF
						165.9795	8	$C_5H_2D_2ONCl_2$	2.9	$C_{12}H_{11}O_2NF_2$
M1	Oxidation	419.0354	$C_{17}H_{15}O_4N_2F_2Cl_2$	−4.2	20	383.0588	7	$C_{17}H_{14}O_4N_2F_2Cl$	−4.4	HCl
						241.0679	100	$C_{12}H_{11}O_3F_2$	2.0	$C_5H_4ON_2Cl_2$
						187.0202	68	$C_8H_5O_3F_2$	0.0	$C_5H_4ON_2Cl_2$, C_4H_6
						179.9620	14	$C_5H_4O_2NCl_2$	3.6	$C_{12}H_{11}O_2NF_2$
						167.0136	3	$C_8H_4O_3F$	−1.8	$C_5H_4ON_2Cl_2$, C_4H_6, HF
Cilomilast		344.1857 (361.2122[a]	$C_{20}H_{26}NO_4$	0.2 0.0	15 20)	**276.1230**	5	$C_{15}H_{18}NO_4$	0.0	C_5H_8
						258.1122	18	$C_{15}H_{16}NO_3$	−1.1	C_5H_8, H_2O
						249.1119	100	$C_{14}H_{17}O_4$	−0.8	C_5H_8, HCN
						230.1170	15	$C_{14}H_{16}NO_2$	−2.5	C_5H_8, H_2O, CO
						203.1063	7	$C_{13}H_{15}O_2$	−1.7	C_5H_8, H_2O, CO, HCN
						198.0907	2	$C_{13}H_{12}NO$	−3.2	C_5H_8, H_2O, CO, CH_3OH
M1	Hydroxylation	360.1803 (377.2068[a]	$C_{20}H_{26}NO_5$	−0.7 0.8	25 25)	342.1705	5	$C_{20}H_{24}NO_4$		H_2O
						276.1231	30	$C_{15}H_{18}NO_4$	0.3	C_5H_8O
						258.1117	28	$C_{15}H_{16}NO_3$	−3.8	C_5H_8O, H_2O
						249.1125	100	$C_{14}H_{17}O_4$	1.6	C_5H_8O, HCN
						230.1183	52	$C_{14}H_{16}NO_2$	3.1	C_5H_8O, H_2O, CO
						203.1071	33	$C_{13}H_{15}O_2$	1.9	C_5H_8O, H_2O, CO, HCN
						198.0927	18	$C_{13}H_{12}NO$	0.0	C_5H_8O, H_2O, CO, CH_3OH

CE, collision energy (eV).
[a]Ammonium adduct.

Rapid Communications in Mass Spectrometry

a 50 mM phosphate buffer at pH 7.4, containing 5 mM $MgCl_2$. In order to differentiate metabolic reactions from incubation/sample preparation artifacts, a substrate blank, a co-factor blank, and an enzyme blank were prepared with each batch of specimens. Phase I metabolism was initiated by addition of NADPH (5 mM) as a co-factor and incubation at 37 °C. The reactivity of enzymes was terminated by adding 200 µL of ice-cold acetone and the generated particulate was removed by centrifugation at 17 000 *g* and 4 °C for 5 min. The supernatant was transferred to a fresh test tube and the acetone removed in a vacuum centrifuge. After another centrifugation at 17 000 *g* for 5 min, the supernatant was diluted by 1:5 with 2% aqueous acetic acid before analysis by LC/ESI-MS/MS.

Urine sample preparation

In order to implement rolipram, roflumilast, cilomilast, and respective phase-I metabolites into current sports drug testing programs, the fitness-for-purpose of an existing initial test method for various doping agents including steroidal compounds, beta-receptor blocking agents, cannabinoids, etc., was evaluated.[18,19] In brief, the procedure requires 3 mL of urine, which is enriched with the internal standard (IS) methyltestosterone before undergoing enzymatic hydrolysis of glucurono-conjugates accomplished with β-glucuronidase from *E. coli*. The resulting aglycons are liquid–liquid extracted (pH 9.6) into *tert*-butyl methyl ether, the organic layer is concentrated to dryness and the dry residue reconstituted in mobile phase for LC/MS/MS analysis (*vide supra*).

For proof-of-concept analysis, a urine sample was obtained from an inpatient receiving roflumilast (Daxas®, 500 µg/day) 4.5 h after ingestion. The patient was informed about the purpose of the study and written consent was provided.

Assay characteristics

Routine doping control measurements were conducted using the above-mentioned established screening platform and the assay's performance concerning specificity, recovery, intraday and interday precision, linearity, and limit of detection (LOD) was characterized for the intact drugs rolipram, roflumilast, and cilomilast. In the absence of certified reference materials for relevant metabolites, the therapeutics served as surrogates and target compounds allowing the assessment of the suitability of the method for sports drug testing purposes according to relevant guidelines.[20]

Lower limit of detection

The lower limit of detection (LLOD) was defined with a signal-to-noise ratio >3 for each analyte with at least two different characteristic ion transitions. Samples were spiked at 5 ng/mL with rolipram, roflumilast, and cilomilast, and LLODs were estimated from signal intensities obtained and blank urine sample noise abundances at corresponding retention times.

Recovery

The recovery of rolipram, roflumilast, and cilomilast from human urine by liquid–liquid extraction (LLE) was determined at 200 ng/mL. Six blank urine samples were fortified with target analytes before sample preparation, and another six blank urine specimens were extracted according to the described protocol followed by addition of 600 ng of each PDE4 inhibitor to the ether layer. For both sets of samples, the IS was spiked into the ether extract and the recovery was calculated by comparison of mean peak area ratios of analyte and IS of samples fortified prior to and after LLE.

Intraday and interday precision

On one day, six urine samples of low (10 ng/mL), medium (50 ng/mL), and high (250 ng/mL) concentrations of all three analytes were prepared and analyzed, and the intraday precision was calculated for each concentration level. On the following day, another set of 18 (6 + 6 + 6) spiked urine samples was prepared and analyzed, and the combined data of days 1 and 2 were evaluated to provide the information required to calculate the interday precisions.

Specificity

Ten different blank urine specimens obtained from 3 female and 7 male healthy volunteers were prepared as described above in order to probe for interfering peaks in the LC/MS/MS chromatograms at expected retention times of the target analytes.

Linearity

Calibration curves ranging from 10 to 1000 ng/mL were prepared from spiked urine samples to allow the assumption of a linear correlation between urinary analyte concentration and measured signal intensity.[21]

Ion suppression/enhancement effects

Tests for ion suppression/enhancement effects were conducted at 100 ng/mL using either solvents A/B (1:1, v/v) or extracts of blank urine samples prepared according to the above reported procedure. Three different blank urine specimens were analyzed and peak intensities observed for the three target compounds were compared with those found with the standard solution at 100 ng/mL.

RESULTS AND DISCUSSION

Mass spectrometry of PDE4 inhibitors and *in vitro* generated metabolites

All target compounds were studied by high-resolution/high-accuracy mass spectrometry, MS^3 experiments, and, where considered relevant, by H/D exchange and MS. The main results are summarized in Table 1 and dissociation pathways of active drugs and corresponding metabolites are presented in the following.

Mass spectrometry – rolipram and main metabolites

The product ion mass spectrum of rolipram as generated from the protonated molecule $[M+H]^+$ at *m/z* 276 by collisional activation is depicted in Fig. 2(a). The main product ions are observed at *m/z* 208, 191, 176, 163, 131, and 103, most of which are produced consecutively as studied and demonstrated by MS^3 experiments. The loss of

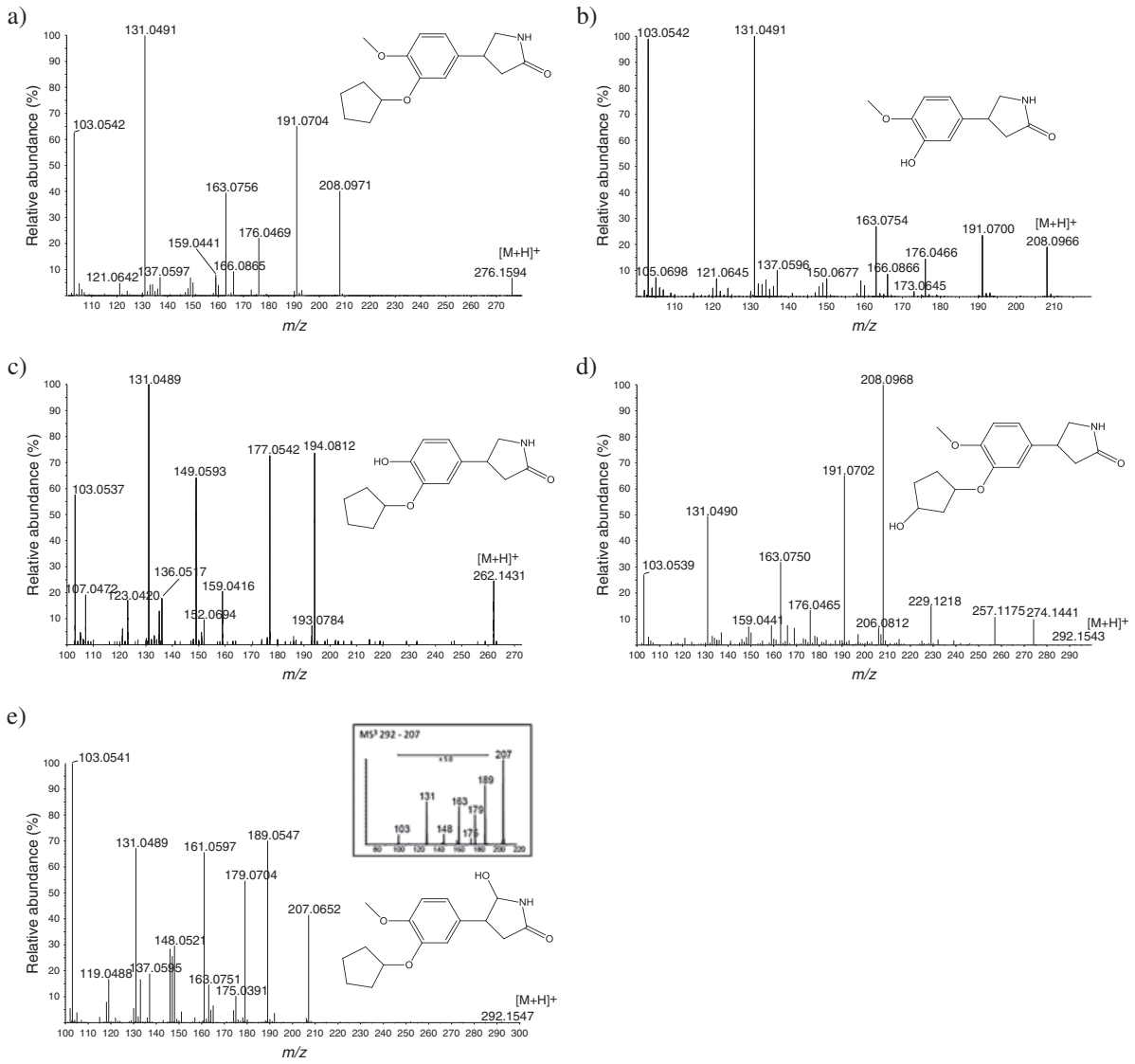

Figure 2. Product ion mass spectra of protonated precursor ions $[M+H]^+$ of (a) *m/z* 276 of rolipram, (b) *m/z* 208 of decyclopentylated rolipram, (c) *m/z* 262 of demethylated rolipram (M2), and (d) and (e) *m/z* 292 of hydroxylated rolipram (M3 and M5/M6, respectively).

cyclopentene (68 u) from *m/z* 276 is suggested to yield the ion at *m/z* 208 that subsequently eliminates ammonia from the pyrrolidin-2-one residue to produce the ion at *m/z* 191, as supported by accurate mass and MS^3 measurements. The release of ammonia requires substantial rearrangements within the protonated pyrrolidinone core including the migration of a hydrogen atom from C-4″ to N-1″ and formation of a C–C bond between C-3″ and C-5″ that eventually leads to a proposed cyclobutanone moiety (Scheme 1(a)). The resulting ion at *m/z* 191 was shown to give rise to product ions at *m/z* 176 (−15 u) and 163 (−28 u), which were attributed to the losses of a methyl radical and carbon monoxide, respectively, as corroborated by their accurate masses and illustrated in Scheme 1(a). The methoxy group of *m/z* 163 is further suggested to be eliminated as methanol to form the base peak of the product ion mass spectrum at *m/z* 131, possibly bearing a quinone-like structure as generated via an epoxide intermediate. Finally, *m/z* 131 was found to produce *m/z* 103 by releasing carbon monoxide, which presumably represents the cation of 5-cyclopropylidene-cyclopenta-1,3-diene (Scheme 1(a)). Based on these site-specific fragmentation pathways, main phase-I metabolites of rolipram were identified from *in vitro* assay samples according to published human *in vivo* data.[11,12] By means of radiolabeling studies it was demonstrated that approximately 60% of the entire radioactivity is excreted into urine within 48 h, mainly as dealkylated (M1 and M2), regioisomerically cyclopentyl-hydroxylated (M3 and M4), and stereoisomerically pyrrolidinone-hydroxylated (M5 and M6) rolipram. These structures were also detected following *in vitro* incubations of the drug and representative product ion mass spectra of M1, M2, M3, and M5/M6 are depicted in Figs. 2(b)–2(e). The dissociation pathway of $[M+H]^+$ at *m/z* 208 of M1 is identical to that of rolipram (after gas-phase CID generating *m/z* 208 as a product ion) and abundant and diagnostic product ions are found at *m/z* 191, 163, 131, and 103 as shown in Fig. 2(b). In the case of M2 (Fig. 2(c)), most of the abundant product ions are decremented by 14 u, except for *m/z* 131 and 103, which

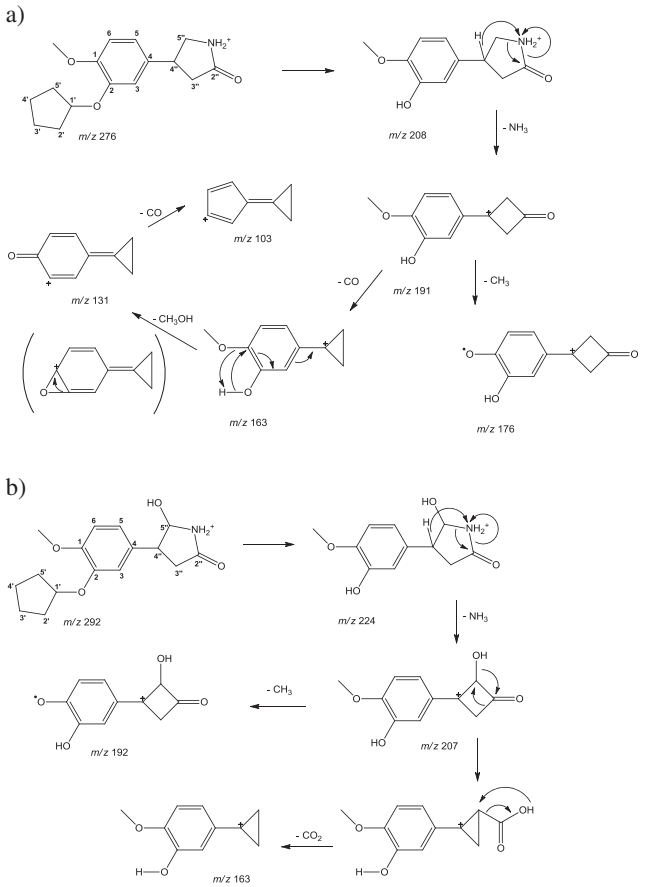

Scheme 1. Proposed dissociation pathways of (a) rolipram and (b) M5/M6 of rolipram under positive ESI/CID conditions.

are suggested to comprise the same structures as those obtained from the intact drug due to elimination cascades eventually yielding identical product ions. In a similar manner, M3 gives rise to numerous product ions identical to those found in the product ion mass spectrum of rolipram, as the hydroxylated cyclopentyl residue is immediately eliminated from the protonated precursor ion (*m/z* 292) forming the common product ion at *m/z* 208 (Fig. 2(d)). Locating the hydroxyl function at C-5″ results in a significantly altered product ion mass spectrum as illustrated for M5/M6 in Fig. 2(e). In agreement with the aforementioned losses of cyclopentene (−68 u) and ammonia (−17 u) from the protonated precursor ion at *m/z* 292, it is suggested that the ion at *m/z* 207 is generated, corresponding to *m/z* 191 of rolipram. While the subsequent elimination of carbon monoxide is also observed with M5/M6 (giving rise to *m/z* 179), the hydroxylated metabolite further releases water (−18 u) to yield the ions at *m/z* 189 (from *m/z* 207) and 161 (from *m/z* 179). Notably, the ions at *m/z* 163, 131, and 103 remain in the product ion mass spectrum despite the assumption that the hydroxylated atom C-5″ is present in all of them. This is explained by a second dissociation pathway (evidenced by MS^3 experiments; data shown as inset in Fig. 2 (e)) starting with the fragmentation of *m/z* 207 that eliminates carbon dioxide (−44 u) instead of carbon monoxide and, thus, generates *m/z* 163 as found with rolipram (Scheme 1(b)). Consequently, the subsequently produced ions (i.e. *m/z* 131 and 103) are also detected in the case of M5/M6.

Mass spectrometry – roflumilast and main metabolite

The halogenated analyte roflumilast and its main metabolite roflumilast-N-oxide as well as their fivefold deuterated analogs were measured by LC/ESI-MS/MS by Knebel *et al.* in 2012 and dissociation routes and product ion structures were suggested based on low-resolution MS/MS spectra.[15] Complementary to these results, high-resolution/high-accuracy MS and H/D exchange data were generated in the present study and dissociation pathways were revisited in the light of the additional information obtained. The protonated precursor ion $[M+H]^+$ of roflumilast is observed at *m/z* 403 and predominantly dissociates into three abundant (*m/z* 241, 187, and 164) and three less intense (*m/z* 367, 349, and 167) product ions as illustrated in Fig. 3(a). By means of accurate mass determinations, the generation of *m/z* 367 and 348 was readily attributed to the losses of HCl (36 u) and C_4H_6 (54 u, methylenecyclopropane) potentially via the fragmentation routes depicted in Scheme 2. The abundant ion at *m/z* 241 was, in agreement with Knebel *et al.*, attributed to the cleavage of the amide bond, yielding an even-electron (3-(cyclopropylmethoxy)-4-(difluoromethoxy) phenyl)(oxo)methylium ion that subsequently eliminates methylenecyclopropane (54 u) to form the corresponding even-electron (4-(difluoromethoxy)-3-hydroxyphenyl)(oxo) methylium ion at *m/z* 187 (Scheme 2) as studied in MS^3 experiments. The structural elucidation of *m/z* 164 represented a major challenge as accurate mass measurements suggested an elemental composition of $C_5H_4ONCl_2$, which necessitates the migration of an oxygen atom and the addition of a hydrogen atom and a proton to the dichloropyridine moiety of roflumilast. Considering the fact that protons are regarded

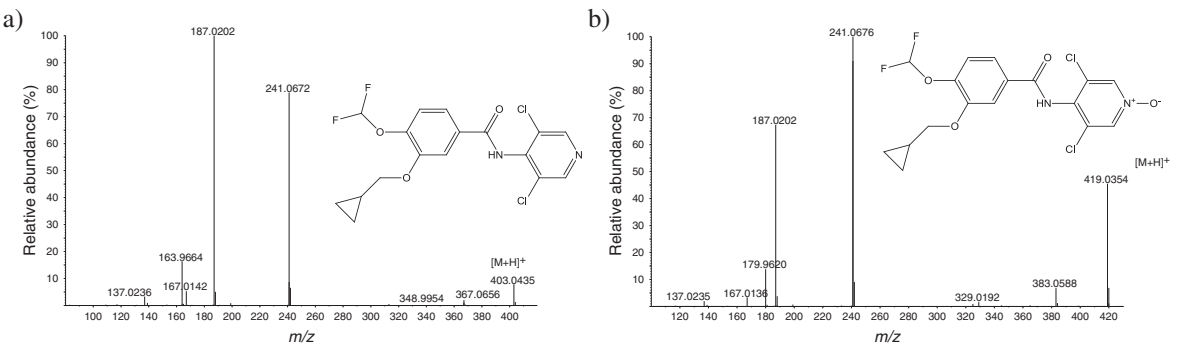

Figure 3. Product ion mass spectra of protonated precursor ions $[M+H]^+$ of (a) *m/z* 403 of roflumilast and (b) *m/z* 419 of roflumilast-N-oxide.

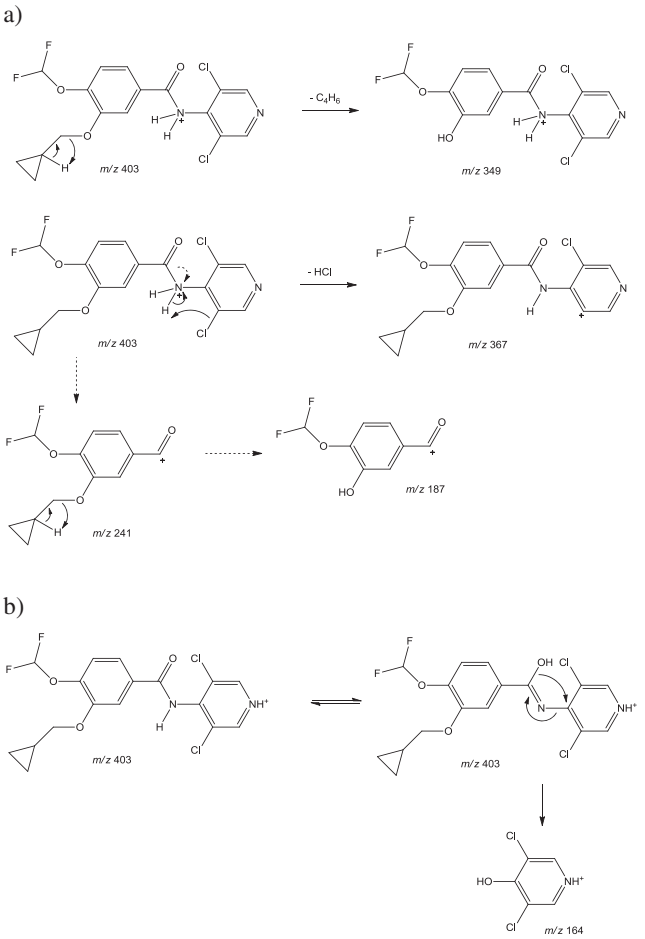

Scheme 2. Proposed dissociation pathways of roflumilast under positive ESI/CID conditions.

as mobile in conjugated electron systems and particularly under CID conditions,[22] locating the proton at the pyridine nucleus (e.g. at the nitrogen atom) is conceivable. The imidic acid tautomer of the amide function can then eliminate 3-(cyclopropylmethoxy)-4-(difluoromethoxy)benzonitrile as illustrated in Scheme 2(b), giving rise to the 3,5-dichloro-4-hydroxypyridin-1-ium ion (*m/z* 164) under transfer of the hydroxyl function. Using H/D exchange and ionization in deuteroxide/deuterated methanol, the retention of two deuterium atoms (one from H/D exchange at the amide group and one from the ionization process) in the ion at *m/z* 164 was observed (Table 1), which caused a shift to *m/z* 166 and thus further corroborated the proposed fragmentation route. The product ion mass spectrum of protonated roflumilast N-oxide, the main metabolite of the COPD therapeutic, is shown in Fig. 3(b). In accordance with the above postulated dissociation pathways, ions are either incremented by 16 u due to the introduction of an oxygen atom (e.g. *m/z* 419, 383, 364, and 180) or maintained due to their composition that lacks the dichloropyridine residue (e.g. *m/z* 241 and 187).

Mass spectrometry – cilomilast and main metabolites

Close structural relationship is observed between rolipram (**2**, *vide supra*) and cilomilast (**4**). Consequently, common but also unique dissociation routes of the protonated molecules of both analytes are observed and the product ion mass spectrum of $[M+H]^+$ (*m/z* 344) of **4** is depicted in Fig. 4(a). In agreement with **2**, the $[M+H]^+$ ion of **4** eliminates cyclopentene (68 u), which yields the product ion at *m/z* 276 that subsequently follows several different fragmentation pathways as illustrated in Scheme 3. The loss of water (18 u) results in the ion at *m/z* 258 that further releases CO (−28 u) to produce *m/z* 230 as supported by MS^3 experiments; the ion at *m/z* 230, however, also might be the result of the loss of formic acid (46 u, solid arrows) from *m/z* 276. The ion at *m/z* 276 also eliminates HCN (27 u, dashed arrows) yielding the base peak of the product ion mass spectrum at *m/z* 249, which was found to produce *m/z* 203 by the subsequent loss of formic acid (46 u) or the consecutive releases of water and CO. In addition, the loss of methanol (32 u) from *m/z* 230 was observed, resulting in the low abundance product ion at *m/z* 198. According to literature data, main phase-I metabolites of cilomilast are 3-hydroxylated at the cyclopentyl moiety or dealkylated by removal of the cyclopentyl residue.[10] Using the employed *in vitro* methods, only the hydroxylated analog was obtained in amounts sufficient for mass spectrometric studies and the product ion mass spectrum of the protonated metabolite is shown in Fig. 4(b). The presence of the above reported diagnostic product ions corroborate the structural assignment (i.e. 3-hydroxylation) of the metabolic product.

Doping control analytical assay

Based on the above-reported diagnostic product ions generated from the intact drugs and characteristic phase-I metabolites, an existing doping control analytical assay based

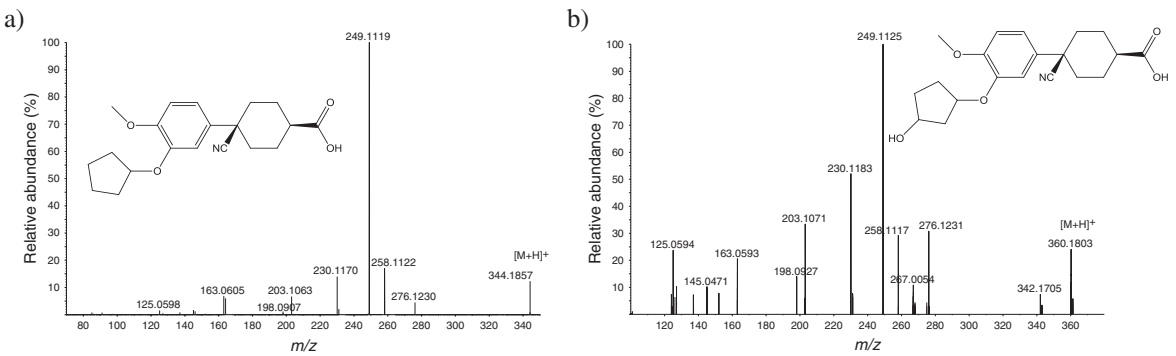

Figure 4. Product ion mass spectra of protonated precursor ions $[M+H]^+$ of (a) *m/z* 344 of cilomilast and (b) *m/z* 360 of hydroxylated cilomilast.

Rapid Communications in Mass Spectrometry

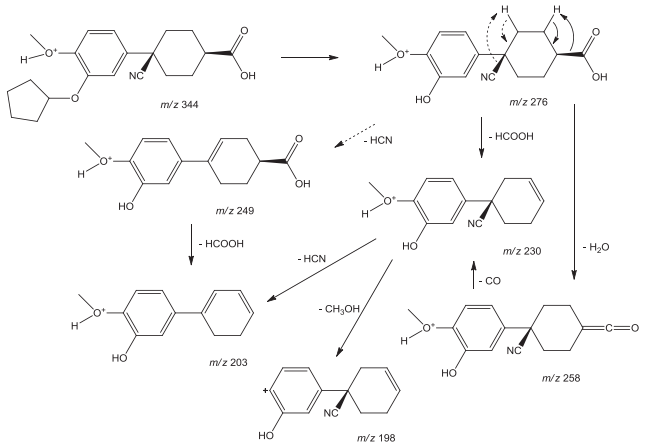

Scheme 3. Proposed dissociation pathways of cilomilast under positive ESI/CID conditions

on LC/QqQ-MS/MS and designed for multi-analyte screening purposes was evaluated concerning its fitness-for-purpose to also detect the PDE4 inhibitors rolipram, roflumilast, and cilomilast.[23] Sports drug testing assays such as the method employed herein commonly focus on phase-I metabolites either excreted unconjugated or liberated from glucuronides by means of respective β-glucuronidases.[18] Hence, on the one hand, the protocol used will (most probably) allow for the cleavage and subsequent analysis of the above-studied and characterized metabolites but, on the other hand, fail to consider sulfate-conjugated compounds, which are of minor significance for cilomilast[10] and roflumilast[15] but of considerable abundance in rolipram elimination studies.[11,12] Although the amount of rolipram metabolites not bearing a sulfate moiety is sufficient to enable adequate drug testing, complementary detection methods targeting intact conjugates, e.g. after solid-phase extraction or direct injection of urine,[24] might provide a valuable addition to the methodological approach presented.

Despite the modest amounts of unmodified therapeutics expected to be renally eliminated after oral administration, the active components were chosen as target/surrogate analytes due to the unavailability of certified reference material of main urinary metabolites.

In Table 2, the assay characteristics are summarized, demonstrating the capability of the method to sensitively and specifically detect the target compounds in human urine. The recoveries of analytes ranged from 20 to 100% and detection limits were estimated between 1 and 5 ng/mL. Intraday and interday precisions were found to range from 1.5 to 18.6% and the chosen ion transitions for each compound enabled their unambiguous detection, generating no interfering signals in blank urine samples at expected retention times. Ion suppression of less than 15% was observed for rolipram and cilomilast, while roflumilast experienced ion enhancement of approximately 24% in the presence of co-extracted urinary matrix components. Typical extracted-ion chromatograms of blank urine samples, spiked specimens containing 10 ng/mL of each compound, and *in vitro* assay samples are illustrated in Fig. 5 for (a) rolipram, (b) roflumilast, and (c) cilomilast. In addition, for roflumilast a post-administration urine sample collected from a COPD patient on roflumilast treatment (4.5 h post-administration of 500 µg of roflumilast) is depicted

Table 2. Summary of assay validation results for the detection of three PDE4 inhibitors in human urine

Compound	LOD (ng/mL)	Recovery (%) at 200 ng/mL (n = 6 + 6)	Linearity (5–1000 ng/mL, $n = 6$)		Intraday precision ($n = 18$)		Interday precision ($n = 18 + 18$)		Ion suppression (−)/ enhancement (+) (%)
					Concentration (ng/mL)	CV (%)	Concentration (ng/mL)	CV (%)	
Rolipram	1	79	Slope	0.27	10	7.7	10	11.5	−14
			Intercept	4.25	50	7.0	50	7.3	
			r^2	0.993	250	8.0	250	14.3	
Roflumilast	1	100	Slope	0.04	10	7.3	10	13.8	−14
			Intercept	−0.50	50	12.3	50	12.0	
			r^2	0.976	250	6.9	250	12.3	
Cilomilast	5	20	Slope	0.007	10	13.7	10	18.6	+24
			Intercept	−0.10	50	4.9	50	10.0	
			r^2	0.981	250	1.5	250	12.4	

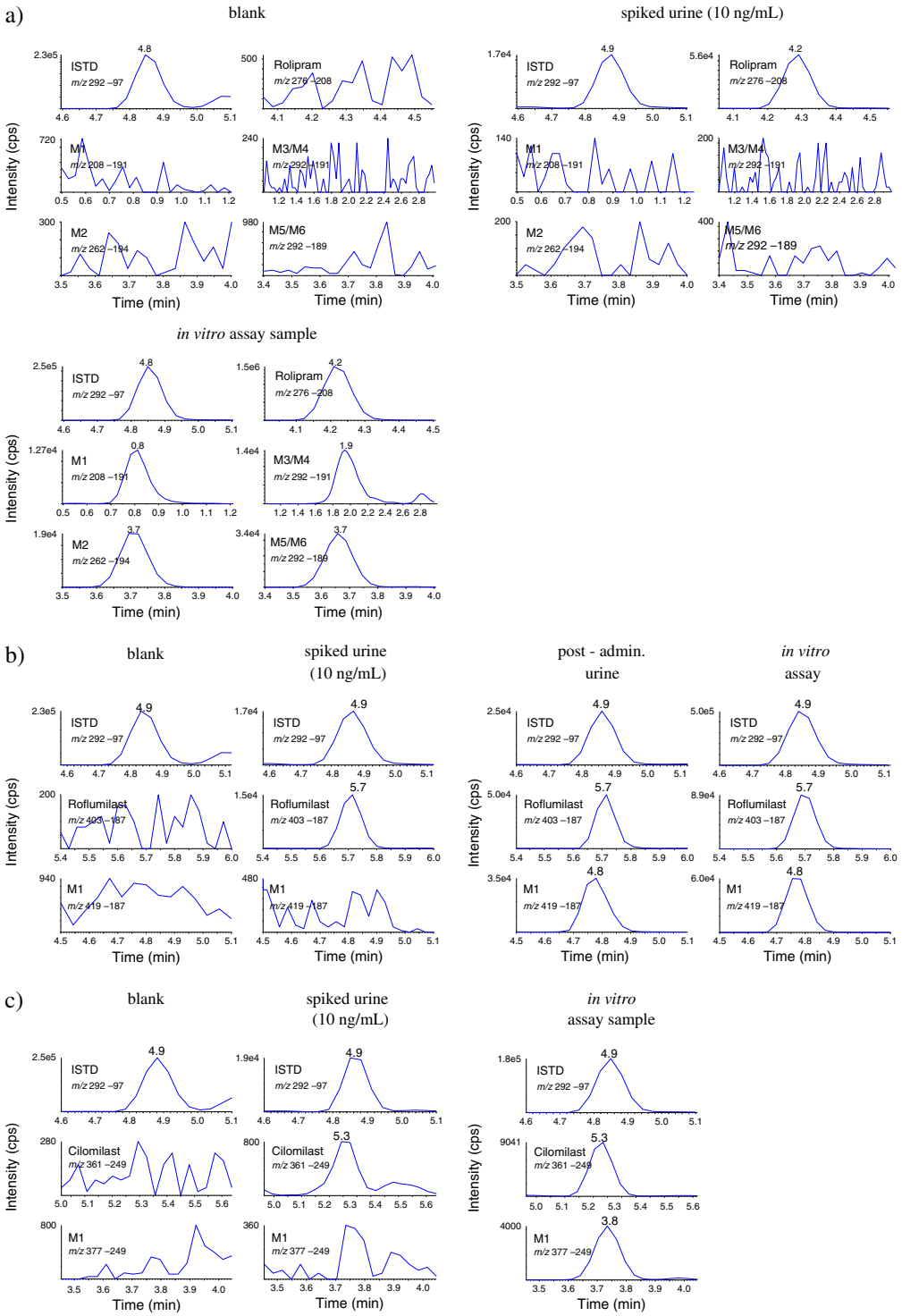

Figure 5. Extracted ion chromatograms of blank urine samples, urines spiked with 10 ng/mL of each drug, and *in vitro* incubation assay specimens of (a) rolipram, (b) roflumilast, and (c) cilomilast. In the case of roflumilast a spot urine sample (4.5 h post-administration) of a patient receiving the PDE4 inhibitor for COPD treatment is also presented, providing the proof-of-concept for the test method.

in Fig. 5(b), demonstrating the capability of the method to detect both the intact compound and the main metabolite using the employed doping control screening procedure. However, the time periods of potential detection windows require additional elimination studies, which were beyond the scope of the present study.

While rolipram and roflumilast demonstrated excellent proton affinities and thus yielded abundant protonated molecules and intense product ions as discussed above, cilomilast yielded substantially fewer precursor ions in both positive and negative ionization modes when considering protonation or deprotonation only. In order to accomplish detection limits

Rapid Communications in Mass Spectrometry

comparable with those of the other PDE4 inhibitors, adduct ion formation promoted by the ammonium acetate added to the mobile phase (A) was exploited and product ions resulting from $[M+NH_4]^+$ of cilomilast at *m/z* 362 and 377 of the corresponding hydroxylated metabolite were used to allow for adequate detection limits for doping control purposes.

CONCLUSIONS

In the present study, the mass spectrometric characterization of three PDE4 inhibitors was elucidated in order to support and accelerate doping control analytical efforts concerning drugs and emerging drug candidates potentially being misused in elite sport. Since urine is the most frequently collected doping control sample matrix, product ion mass spectra of *in vitro* generated phase-I metabolites were also investigated to provide reference spectra and diagnostic precursor-product ion pairs to enable the sensitive detection of these target compounds if required. All three substances have been thoroughly studied earlier concerning their metabolism and renal elimination, but mass spectral information on major metabolites and their traceability for preventive doping control purposes was limited. In the absence of sufficient reference materials of metabolic products of rolipram, roflumilast, and cilomilast, the capability of a routine doping control assay based on targeted LC/MS/MS was assessed by characterizing the test method with the intact therapeutics as structurally relevant substances and surrogates for respective metabolites. In addition, minute amounts of these compounds are expected to be excreted unchanged into urine;[10] hence, the detection of the drug itself in addition to its metabolic products is enabled, as demonstrated with spiked urine samples as well as an administration study specimen obtained from a COPD patient undergoing roflumilast treatment.

The approved PDE4 inhibitor roflumilast is currently not prohibited according to the WADA 2013 prohibited list;[25] however, the non-approved compounds rolipram and cilomilast are covered by section S0 (non-approved substances) of the anti-doping rules, which highlights an issue that requires attention in future considerations of adjusting the list of prohibited substances and methods of doping. The recent discovery of the effect of PDE4 inhibitors on mitochondrial biosynthesis and resulting performance enhancement in laboratory rodents has fueled concerns about the drugs' misuse potential and proactive and preventive measures are indicated to ensure an efficient and timely anti-doping fight.

Acknowledgements

The study was supported by Antidoping Switzerland (Berne, Switzerland), the Federal Ministry of the Interior of the Federal Republic of Germany (Bonn, Germany), and the Manfred-Donike-Institute for Doping Analysis (Cologne, Germany).

REFERENCES

[1] R. I. Tennen, E. Michishita-Kioi, K. F. Chua. Finding a target for resveratrol. *Cell* **2012**, *148*, 387.
[2] S. J. Park, F. Ahmad, A. Philp, K. Baar, T. Williams, H. Luo, H. Ke, H. Rehmann, R. Taussig, A. L. Brown, M. K. Kim, M. A. Beaven, A. B. Burgin, V. Manganiello, J. H. Chung. Resveratrol ameliorates aging-related metabolic phenotypes by inhibiting cAMP phosphodiesterases. *Cell* **2012**, *148*, 421.
[3] C. A. Blum, J. L. Ellis, C. Loh, P. Y. Ng, R. B. Perni, R. L. Stein. SIRT1 modulation as a novel approach to the treatment of diseases of aging. *J. Med. Chem.* **2011**, *54*, 417.
[4] L. Pages, A. Gavalda, M. D. Lehner. PDE4 inhibitors: a review of current developments (2005–2009). *Exp. Opin. Ther. Patents* **2009**, *19*, 1501.
[5] A. Hatzelmann, E. J. Morcillo, G. Lungarella, S. Adnot, S. Sanjar, R. Beume, C. Schudt, H. Tenor. The preclinical pharmacology of roflumilast–a selective, oral phosphodiesterase 4 inhibitor in development for chronic obstructive pulmonary disease. *Pul. Pharmacol. Ther.* **2010**, *23*, 235.
[6] K. F. Rabe. Update on roflumilast, a phosphodiesterase 4 inhibitor for the treatment of chronic obstructive pulmonary disease. *Br. J. Pharmacol.* **2011**, *163*, 53.
[7] P. Salari, M. Abdollahi. Phosphodiesterase inhibitors in inflammatory bowel disease. *Expert. Opin. Investig. Drugs* **2012**, *21*, 261.
[8] J. M. Michalski, G. Golden, J. Ikari, S. I. Rennard. PDE4: a novel target in the treatment of chronic obstructive pulmonary disease. *Clin. Pharmacol. Ther.* **2012**, *91*, 134.
[9] Z. Diamant, D. Spina. PDE4 inhibitors: a novel, targeted therapy for obstructive airways disease. *Pul. Pharmacol. Ther.* **2011**, *24*, 353.
[10] M. A. Giembycz. Cilomilast: a second generation phosphodiesterase 4 inhibitor for asthma and chronic obstructive pulmonary disease. *Expert. Opin. Investig. Drugs* **2001**, *10*, 1361.
[11] W. Krause, G. Kuhne. Biotransformation of the antidepressant D,L-rolipram. II. Metabolite patterns in man, rat, rabbit, rhesus and cynomolgus monkey. *Xenobiotica* **1993**, *23*, 1277.
[12] W. Krause, G. Kuhne, U. Jakobs, G. A. Hoyer. Biotransformation of the antidepressant DL-rolipram. I. Isolation and identification of metabolites from rat, monkey, and human urine. *Drug Metab. Dispos.* **1993**, *21*, 682.
[13] T. D. Bethke, M. Hartmann, A. Hunnemeyer, G. Lahu, C. H. Gleiter. Influence of renal impairment on the pharmacokinetics of oral roflumilast: an open-label, parallel-group, single-center study. *Int. J. Clin. Pharmacol. Ther.* **2011**, *49*, 491.
[14] T. D. Bethke, G. Lahu. High absolute bioavailability of the new oral phosphodiesterase-4 inhibitor roflumilast. *Int. J. Clin. Pharmacol. Ther.* **2011**, *49*, 51.
[15] N. G. Knebel, R. Herzog, F. Reutter, K. Zech. Sensitive quantification of roflumilast and roflumilast N-oxide in human plasma by LC-MS/MS employing parallel chromatography and electrospray ionisation. *J. Chromatogr. B* **2012**, *893–894*, 82.
[16] S. Beuck, W. Bornatsch, A. Lagojda, W. Schänzer, M. Thevis. Development of liquid chromatography-tandem mass spectrometry-based analytical assays for the determination of HIF stabilizers in preventive doping research. *Drug Test. Anal.* **2011**, *3*, 756.
[17] S. Beuck, W. Schänzer, M. Thevis. Investigation of the in vitro metabolism of the emerging drug candidate S107 for doping-preventive purposes. *J. Mass Spectrom.* **2011**, *46*, 112.
[18] M. Thevis. *Mass Spectrometry in Sports Drug Testing – Characterization of Prohibited Substances and Doping Control Analytical Assays*. John Wiley, Hoboken, **2010**.
[19] M. Thevis, S. Guddat, W. Schänzer. Doping control analysis of trenbolone and related compounds using liquid chromatography-tandem mass spectrometry. *Steroids* **2009**, *74*, 315.
[20] International Conference on Harmonisation, **2004**. http://www.fda.gov/Drugs/GuidanceComplianceRegulatoryInformation/Guidances/ucm265700.htm (accessed 7 March 2013).

[21] J. Mandel. *The Statistical Analyses of Experimental Data*. John Wiley, New York, **1964**.
[22] V. H. Wysocki, G. Tsaprailis, L. L. Smith, L. A. Breci. Mobile and localized protons: a framework for understanding peptide dissociation. *J. Mass Spectrom.* **2000**, *35*, 1399.
[23] U. Mareck, M. Thevis, S. Guddat, A. Gotzmann, M. Bredehöft, H. Geyer, W. Schänzer, in *Recent Advances in Doping Analysis*, vol. 12, (Eds: W. Schänzer, H. Geyer, A. Gotzmann, U. Mareck). Sport und Buch Strauss, Cologne, **2004**, p. 65.
[24] M. Thevis, A. Thomas, W. Schänzer. Current role of LC-MS (/MS) in doping control. *Anal. Bioanal. Chem.* **2011**, *401*, 405.
[25] World Anti-Doping Agency, **2013**. http://www.wada-ama.org/en/World-Anti-Doping-Program/Sports-and-Anti-Doping-Organizations/International-Standards/Prohibited-List/ (accessed 7 January 2013).

